106–113 *Nucleic Acids Research, 2005, Vol. 33, No. 1*
doi:10.1093/nar/gki154

Effects of camptothecin on double-strand break repair by non-homologous end-joining in DNA mismatch repair-deficient human colorectal cancer cell lines

Sandrine Jacob, Catherine Miquel, Alain Sarasin and Françoise Praz*

Centre National de la Recherche Scientifique, Unité Propre de Recherche 2169, Genetic Instability and Cancer, Institut Gustave Roussy, 39 rue Camille Desmoulins, 94 800 Villejuif, France

Received October 31, 2004; Revised and Accepted December 8, 2004

ABSTRACT

Loss of a functional mismatch repair (MMR) system in colorectal cancer (CRC) cells is associated with microsatellite instability and increased sensitivity to topoisomerase inhibitors. In this study, we have investigated whether a defect in double-strand break (DSB) repair by non-homologous end-joining (NHEJ) could explain why MMR-deficient CRC cells are hypersensitive to camptothecin (CPT), a topoisomerase I inhibitor. To evaluate the efficiency and the fidelity of DSB repair, we have transiently transfected plasmids containing cohesive or non-complementary ends in cells with various MMR defects. We have observed that the repair efficiency of DSB with cohesive and non-complementary ends is comparable in all cell lines. In contrast to the MMR-proficient cell line HT29, the MMR-deficient cell lines were highly accurate in repairing DSB with cohesive ends, but this characteristic could not be directly assigned to the primary MMR deficiency. Furthermore, CPT treatment had no detectable effect on the repair of cohesive ends but significantly decreased the repair efficiency of non-complementary DSB. In conclusion, although our observations show that DSB repair efficiency by NHEJ decreases upon treatment with CPT, which possibly contributes to its cytotoxicity, it is quite unlikely that it accounts for the hypersensitivity of MMR-deficient cells to topoisomerase inhibitors.

INTRODUCTION

In a previous study, we have found that loss of a functional mismatch repair system (MMR) in colorectal cancer (CRC) cell lines is associated with hypersensitivity to camptothecin (CPT), a topoisomerase I inhibitor, and etoposide, a topoisomerase II inhibitor (1). Germ-line mutations in MMR genes, predominantly *hMSH2* and *hMLH1*, have been identified in 50–70% of patients with hereditary nonpolyposis colorectal cancer (HNPCC) [reviewed in (2,3)]. HNPCC-associated tumors are characterized by high instability in simple repetitive microsatellite sequences. This characteristic phenotype, referred as microsatellite instability (MSI), is also observed in 10–15% sporadic CRC (4,5). Because we have further shown that patients with MSI-CRC are more prone to benefit from chemotherapy with irinotecan, a CPT derivative, we were interested in determining the molecular mechanisms responsible for the increased sensitivity of MSI tumors to this drug (6).

CPT and etoposide both interfere with the catalytic cycle of topoisomerases by stabilizing the covalent complex formed by topoisomerase and cleaved DNA, called cleavage complex (7,8). By increasing the half-life of the cleavage complexes formed by topoisomerase II and DNA, etoposide generates higher levels of double-strand breaks (DSBs). The toxicity of CPT is primarily due to the conversion of single-strand break to DSB during S-phase when the replication fork collides with the cleavage complexes formed by topoisomerase I–DNA and CPT (9). Thus far, little is known about the mechanisms that can remove the cleavage complexes and repair the breaks induced by topoisomerase inhibitors. Yet, the breakage ends produced by topoisomerase inhibitors or ionizing radiation are not directly ligatable and need processing prior to end-joining. Several authors have proposed that homologous recombination, as well as non-homologous end-joining (NHEJ) could participate in the repair of the breaks generated at the sites of DNA lesions induced by topoisomerase inhibitors [reviewed in (9)]. In mammalian cells, DSBs are predominantly repaired by NHEJ, a pathway that relies on DNA–PK, a complex formed by the Ku70/Ku80 heterodimer and a catalytic subunit, DNA–PKcs, a member of the phosphatidylinositol 3-kinase family. The complex Ku is able to bind free

*To whom correspondence should be addressed. Tel: +33 1 42 11 49 58; Fax: +33 1 42 11 50 08; Email: praz@igr.fr

ends without any sequence specificity and this step is essential to recruit DNA–PKcs; subsequently ligase IV and its cofactor, XRCC4, are recruited to perform ligation (10). Several observations have recently emphasized that hypersensitivity to topoisomerase inhibitors may be related to a defect in DSB repair by NHEJ. Mutants for Ku80 or Ku70 are hypersensitive to etoposide, while a defect in DNA–PKcs sensitizes to CPT (11–13).

In addition to repairing base–base mispairs, as well as small insertion or deletion loops arising during DNA replication, some MMR components, including hMSH2, hMSH6 and hMLH1, participate in recombination, DSB repair, apoptosis and cell cycle regulation (14–16). Thus, we undertook this study to define whether DSB repair by NHEJ is impaired in MMR-deficient CRC cell lines. In order to evaluate the efficiency and the accuracy of DSB repair, we have transiently transfected a plasmid linerarized with restriction enzymes generating cohesive ends or non-complementary ends in a panel of CRC cell lines with various defects in MMR. Our results show that (i) the DSB repair efficiency of either cohesive or non-cohesive ends is not affected by a defect in MMR, (ii) the accuracy of end-joining is significantly higher in MMR-deficient cell lines, a characteristic that nevertheless persists in MMR-complemented cell lines and (iii) treatment with CPT significantly decreases the repair efficiency of DSB with non-cohesive ends in all cell lines. In conclusion, our observations rule out the possibility that the hypersensitivity of MMR-deficient CRC cell lines to topoisomerase inhibitors occurs as a consequence of defective DSB repair by NHEJ.

MATERIALS AND METHODS

Cell lines

We have used six different cell lines that are proficient or not for MMR: HT29 (MMR+), LoVo (*hMSH2*−), HCT116 (*hMLH1*−), mlh1-2 (*hMLH1*-complemented HCT116), DLD1 (*hMSH6*−) and DLD1-ch2 (*hMSH6*-complemented DLD1) (see Supplementary Material). With the exception of LoVo, all cell lines were grown in monolayer cultures in DMEM supplemented with penicillin (100 μg/ml), streptomycin (100 U/ml), L-glutamine (2 mM) and 10% heat-inactivated fetal calf serum (FCS). LoVo was grown in monolayer cultures in a mixture composed of DMEM and Ham's F-12 (v/v) supplemented as for DMEM. The mlh1-2 cell line obtained by transfecting the *hMLH1*-deficient HCT116 cell line with a wild-type *hMLH1*-expression vector was continuously grown in the presence of hygromycin (100 μg/ml) (1). The DLD1-ch2, a kind gift from Thomas Kunkel, obtained by introducing the entire chromosome 2 tagged with the neomycin resistance gene, was grown in the presence of G418 (600 μg/ml) (17).

Plasmid preparation

The pHRecSJ plasmid used in the *in vivo* cell end-joining assay contains the prokaryotic ColEI origin and the β-*lactamase* gene (AmpR), and was kindly given by Dora Papadopoulo (18). The plasmid was linearized with restriction enzymes that recognize a unique site within the substrate: EcoRI [5′-protruding single stranded (PSS) cohesive ends], ApaI (3′-PSS cohesive ends) or both enzymes together (non-complementary ends) (New England Biolabs). The completeness of the digestion was assessed by transforming linearized substrates into XL1-blue *Escherichia coli*, and was shown to be >99%. The pEGFP-C1 (Clontech) plasmid containing a bacterial replication origin and the gene that confers the resistance to kanamycin was used as a control to monitor the transfection and transformation efficiencies.

Transient transfection and plasmid recovery

All cell lines were transfected by electroporation using an Easyject apparatus (Eurogentec). Exponentially growing cells (3×10^6) were resuspended in culture medium without FCS, supplemented with 20 mM HEPES and electroporated with various amounts of circular (15–500 ng) or linearized (500 ng) pHRecSJ plasmids together with circular pEGFP-C1 (500 ng). The conditions of electroporation were either simple pulse at: 250 V and 1500 μF for HT29; 260 V and 1500 μF for LoVo; 230 V and 1500 μF for DLD1 and DLD1-ch2; or double pulse for HCT116 and mlh1-2, with the first pulse at 1000 V and 25 μF and the second pulse 1 ms later at 100 V and 2500 μF. Forty-eight hours after transfection, plasmids were recovered by a rapid alkaline extraction procedure (19).

Efficiency of DSB repair

Following extraction, lysates were electro-transformed into XL1-blue competent bacteria and plated on Luria–Bertani (LB) plates containing ampicillin (50 μg/ml) or kanamycin (25 μg/ml). The number of bacterial colonies obtained on kanamycin plates was used to normalize the different steps from transfection to plasmid recovery and bacterial transformation. The number of bacterial colonies obtained on ampicillin plates with the different amounts of circular plasmids served to establish a standard curve. The number of bacterial colonies on ampicillin plates obtained with lysates of cells transfected with linearized plasmids allowed us to determine the quantity of plasmids that have been recircularized, using the standard curve. The efficiency of repair was calculated by dividing the quantity of plasmid recircularized versus the quantity of plasmid transfected. The mean percentages of repair efficiency were determined from a minimum of three independent experiments, as indicated in Figures 1 and 4.

Fidelity of DSB repair events

The ratio of error-free and error-prone repair events was determined by screening for the regeneration of the original restriction site. Bacterial colonies were subcultured from ampicillin plates and grown in suspension in 100 μl of LB containing ampicillin (50 μg/ml) at 37°C. After 6 h, 1 μl was used to perform a PCR, using the sense primer: 5′-GCGCGTCCC-ATTCGCCATTCAGGC-3′ and the antisense primer: 5′-CGCCACCTCTGACTTGAGCGTCGA-3′ (corresponding to positions 434–457 and 1565–1588, respectively). PCR was performed in a total volume of 20 μl using 200 μM dNTP (Amersham Pharmacia Biotech, Piscataway) and 0.5 U of *rTaq* DNA polymerase (Amersham Pharmacia Biotech). After an initial 10 min denaturation step at 95°C, amplification was achieved by performing 35 cycles consisting of 1 min denaturation at 95°C, 1 min annealing at 68°C and 2 min elongation at 72°C, followed by a 10 min final elongation step at 72°C.

The PCR products were digested with the enzyme previously used to linearize the plasmids. Briefly, digestion was carried out in a final volume of 40 µl by adding to the entire PCR product 1 U of EcoRI (position 978) or 1 U of ApaI (position 988). After 3 h of incubation at 37°C for EcoRI or 25°C for ApaI, the digestion products were migrated in a 1% agarose gel. The PCR products obtained from accurately repaired plasmids can be recut by the enzyme, giving rise to two bands that can be visualized on the gel, while error-prone repair events cannot be cleaved giving a unique band whose size permits to estimate the size of the deletion. The accuracy of the repair events and the approximate size of the various deletions were determined by analyzing the restriction profile. The deletion sizes were distributed in three groups: small (<50 bp), intermediate (50–500 bp) and large (>500 bp); the assignment accuracy was checked by sequencing 200 error-prone repair events. The mean frequency of accurately repaired DSB was established by analyzing at least three independent experiments per cell line with a minimum of 250 bacterial colonies for each cell type and DSB type.

CPT treatment

A 25 mM stock solution of CPT (Sigma, St Louis) was prepared in dimethyl sulfoxide, aliquoted and kept at −20°C until used. After electroporation with the plasmids, the cells were resuspended in complete medium supplemented with 20 mM HEPES and with CPT at a final concentration of 100 nM.

Detection of frameshift mutations in mononucleotide repeats

Frameshift mutations located in the mononucleotide repeated sequences of *BRCA1* (poly-A8), *BRCA2* (poly-A8), *ATR* (poly-A10), *DNA–PKcs* (poly-A10), BLM (poly-A9), *MRE11* (poly-T11) and *RAD50* (poly-A9) were detected on PCR products performed on ∼50 ng genomic DNA using HotStarTaq DNA Polymerase (Qiagen, Germany) and the following oligonucleotides: 6-FAM-labeled-5′-AGCCCACCTAATTG-TACTG-3′ and 5′-CCATGAGTTGTAGGTTTCTG-3′ for BRCA1; 6-FAM-labeled-5′-TTGCTCACAGAAGGAGGA-CT-3′ and 5′-GCATTTGCTTCAAACTGGGCT-3′ for BRCA2; HEX-labeled-5′-TCTTCTGTAGGAACTTGAAA-GCC-3′ and 5′-TGAAAGCAAGTTTTACTGGACTAGG-3′ for ATR; HEX-labeld-5′-GAAGTTCTAGACTCATGGATG-3′ and 5′-GTGCATCTCACCTGTATCTGG-3′ for DNA–PKcs; 6-FAM-labeled-5′-CTCTGCCACCAGGAAGAATC-3′ and 5′-ACAGCAGTGCTTGTGAGAAC-3′ for BLM; HEX-labeled-5′-AATATTTTGGAGGAGAATCTTAGGG-3′ and 5′-AATTGAAATGTTGAGGTTGCC-3′ for MRE11; and NED-labeled-5′-AACTGCGACTTGCTCCAGAT-3′ and 5′-CAAGTCCCAGCATTTCATCA-3′ for RAD50. Amplification consisted in a 15 min step at 95°C, followed by 50 cycles of 30 s at 96°C, 30 s at 55°C, 30 s at 72°C and a final extension step of 5 min at 72°C. Adequate dilutions of the fluorescent PCR products were mixed with formamide and GS-HD400-ROX molecular weight standards, heat-denaturated and run on a short capillary containing GS Performance Optimized Polymer 4, at a voltage of 15 kV on the ABI 310 Genetic Analyzer using the GeneScan 3.2 software (Applied Biosystems).

RESULTS

Rejoining efficiency through NHEJ in MMR-deficient and MMR-proficient cell lines

Using an *in vivo* plasmid-based assay, we have determined the ability of the various cell lines to repair DSB with cohesive 3′-PSS or 5′-PSS ends, or with non-complementary ends. Histograms shown in Figure 1 represent the mean percentages of the repair efficiency established from a minimum of three independent experiments. As shown in Figure 1, we have observed significant differences in the repair efficiency within the cell lines tested, for 3′-PSS ($P < 0.001$), 5′-PSS ($P = 0.001$)

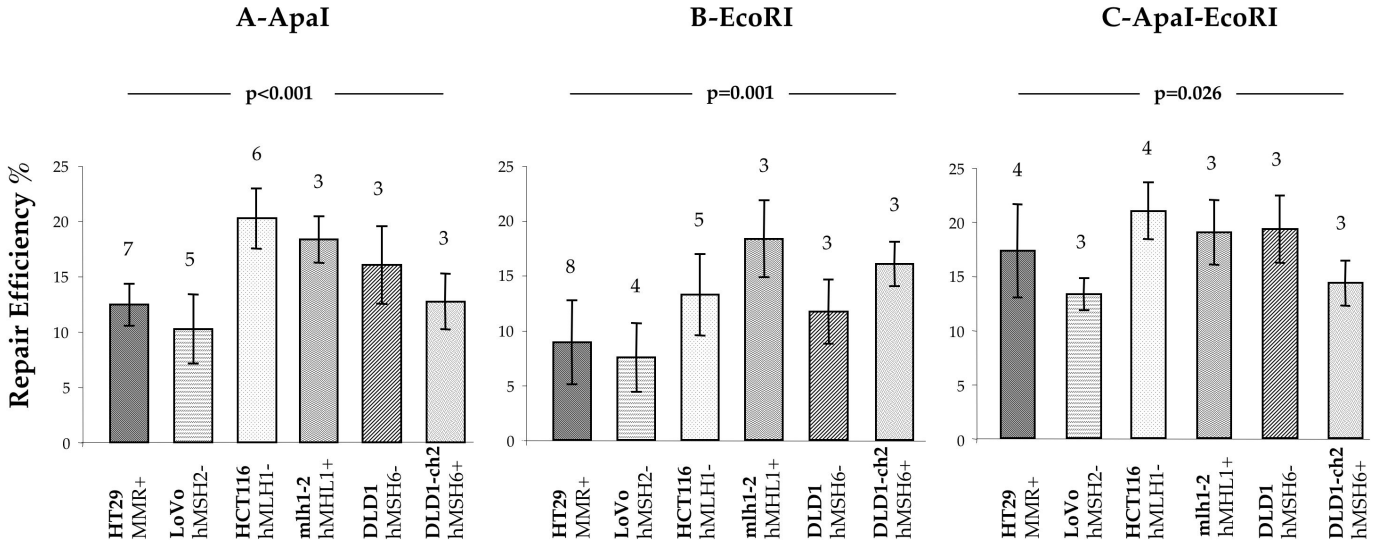

Figure 1. End-joining efficiency of DSB repair by NHEJ in MMR-deficient and MMR-proficient CRC cell lines. Histograms represent the mean percentage of repair efficiency established from a minimum of three independent experiments using plasmids linearized with ApaI (**A**), EcoRI (**B**) and ApaI-EcoRI (**C**). The number of independent experiments is shown above each histogram. The *P* values refer to the comparison of all cell lines.

and non-complementary ends (P = 0.03). As shown in Figure 1A, the repair efficiency of ApaI-induced 3′-PSS DSB was the highest in HCT116 (20.2%) and the lowest in LoVo (10.5%) ($P < 0.001$). The average repair efficiency of 3′-PSS for all the cell lines tested was 15 ± 3.3%. The lowest repair efficiency of the EcoRI-linearized plasmid was again observed for LoVo while mlh1-2, the *hMLH1*-complemented HCT116, was the most efficient cell line (7.5 versus 18.3%, $P = 0.002$), with an average repair efficiency of 12.6 ± 4.1% for all cell lines (Figure 1B). As shown in Figure 1C, LoVo again displayed the lowest efficiency of repair of plasmids with non-complementary ends and HCT116 the highest level (13.3 versus 21%, $P = 0.001$), with an average efficacy of 17.4 ± 3%. Whatever substrates tested, there were no significant differences in the efficiency of repair between HCT116 and mlh1-2, its *hMLH1*-complemented cell line (P = 0.31 for 3′-PSS, P = 0.08 for 5′-PSS and P = 0.37 for non-complementary ends). Similarly, there were no significant differences between DLD1 and DLD1-ch2, its *hMSH6*-corrected derived cell line, in which end-joining efficiencies were 16.0 versus 12.7% for 3′-PSS ($P = 0.22$), 11.7 versus 16% for 5′-PSS ($P = 0.07$) and 19.3 versus 14.3% for non-cohesive ends (P = 0.05). Altogether, these results rule out the hypothesis of a direct link between the efficiency of DSB repair and the primary defect in MMR. This is further reinforced by the fact that HT29 (MMR-proficient) and LoVo (*hMSH2*-deficient) are the two cell lines that showed the lowest levels of repair of DSB with either 5′- or 3′-PSS. Comparing the repair efficiency of ApaI- and EcoRI-induced DSB indicated that, with the exception of HCT116, no cell line displayed significant differences in their ability to repair 5′-PSS and 3-PSS DSB. Nevertheless, with the exception of DLD1-ch2, the 5′-PSS DSBs were slightly less efficiently repaired, and the substrates with non-complementary ends were the most efficiently rejoined. Thus, these observations exclude the possibility that a defect in MMR directly affects the ability of cells to repair DSB with either 5′-PSS or 3′-PSS cohesive ends or with non-complementary ends.

Rejoining fidelity through NHEJ in MMR-deficient and MMR-proficient cell lines

Histograms shown in Figure 2 represent the mean frequency of the error-free events obtained after repair of the various DSBs. Interestingly, we have observed a strong difference in the end-joining fidelity of complementary ends between the MMR-proficient HT29 cell line and all other cell lines that were very accurate in repairing both 3′-PSS and 5′-PSS cohesive ends ($P < 0.001$ for both ApaI- and EcoRI-linearized plasmids) (Figure 2A and B). Yet, in HT29, the end-joining accuracy was 52.2 and 48% for ApaI- and EcoRI-linearized plasmids, respectively, which is much lower than in HCT116 where error-free repair was performed in 84 and 94.3% of events ($P < 0.001$) (Figure 2A and B). For 3′-PSS, HT29 showed the lowest end-joining fidelity and mlh1-2 the highest, with 52.2 versus 93.3% error-free events ($P < 0.001$). Whereas HCT116 showed a repair accuracy of 84% that is statistically different when compared with mlh1-2, its complemented counterpart (P = 0.04), we did not observe statistically significant differences between DLD1 and DLD1-ch2, with 71.3 versus 72.7% error-free events ($P = 0.64$). For 5′-PSS, HT29 again showed the lowest accuracy of repair with 48% and HCT116 the highest with 94.3%, a statistically significant difference ($P = 0.02$). As for 3′-PSS, there was a statistically significant difference between HCT116 and mlh1-2 (94.3 versus 88%, $P = 0.01$), and no significant differences between DLD1 and DLD1-ch2 (P = 0.80). Thus, in our experiments, the repair accuracy of DSB with complementary ends is similar for 3′- and

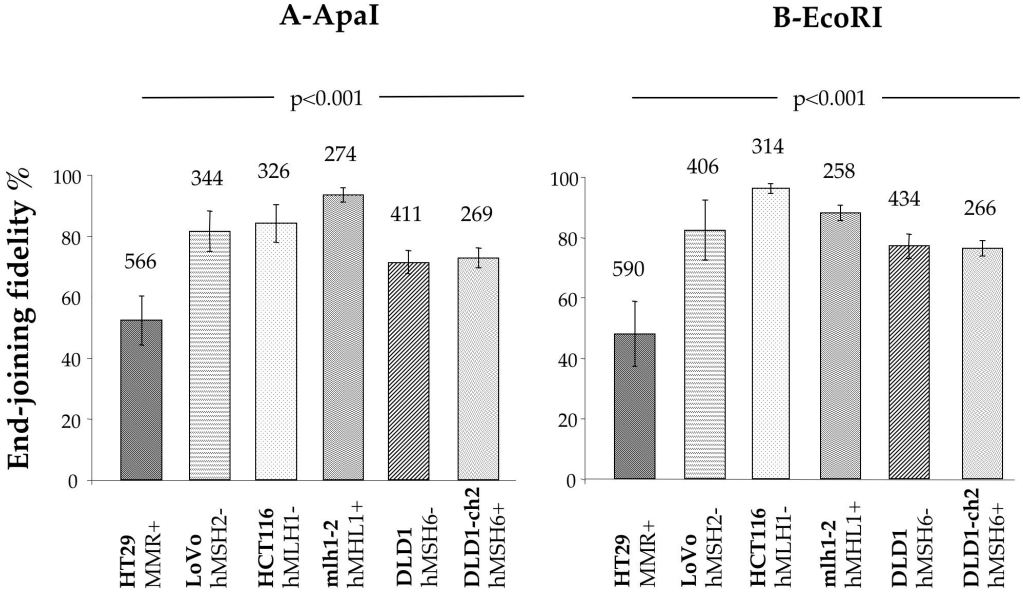

Figure 2. End-joining fidelity of DSB repair by NHEJ in MMR-deficient and MMR-proficient CRC cell lines. Histograms represent the mean frequency in percentage of the error-free events after repair of DSB induced by ApaI (**A**) or EcoRI (**B**) established from a minimum of three independent experiments and a minimum of 250 bacterial colonies analyzed. The numbers of bacterial colonies analyzed are specified above the histograms for each CRC cell lines tested. The P values refer to the comparison of all cell lines.

5′-overhanged PSS but differs significantly between the MMR-proficient HT29 cell lines and the other cell lines tested. Furthermore, deletions associated with NHEJ events in HT29 were strikingly larger than in any of the MMR-deficient cell lines ($P < 0.0001$) (Figure 3). In HT29, deletions >500 bp represented 48% of the events, while their frequency varied from 16% for LoVo and HCT116 to 25% for DLD1 (Figure 3).

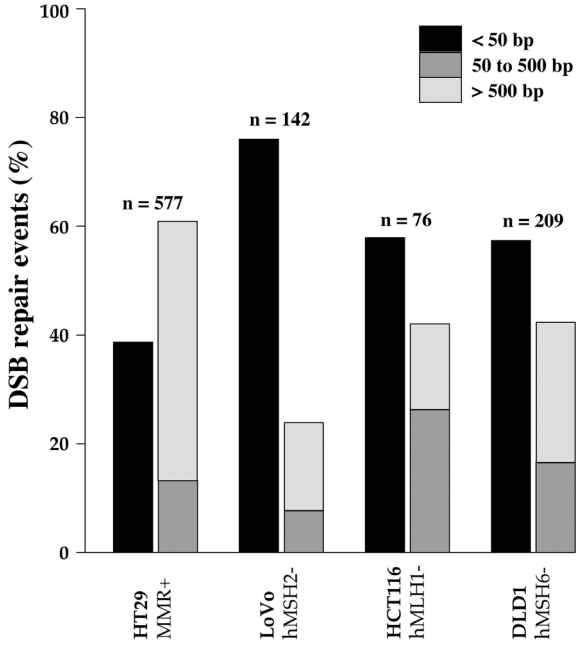

Figure 3. Sizes of the deletions occurring during DSB repair by NHEJ of plasmids with cohesive ends. Shown are the percentages of events with small (<50 bp), intermediate (50–500 bp) or large (>500 bp) deletions, determined after migration on a 1% agarose gel. *n* represents the number of events scored for each cell line. The differences between HT29 and the MMR-deficient cell lines were compared using the Chi2 test ($P < 0.0001$ for all three cell lines).

The repair events displaying small deletions represented <40% in HT29, 60% in HCT116 and DLD1 and reached 76% in LoVo (Figure 3). Thus, in the MMR-deficient cell lines, the repair process is less often error-prone than in HT29, and involves smaller deletions.

Effects of CPT treatment on DSB repair in CRC

In order to test whether CPT affects DSB repair, we have performed the same experiments in cells treated with CPT. Histograms shown in Figure 3 represent the mean percentages of repair efficiency established from a minimum of three independent experiments. As shown in Figure 4A, the CPT-induced decrease in repair efficiency of ApaI-induced DSB was mild for HCT116 (20.2 versus 18.5%, $P = 0.3$) and for LoVo (10.2 versus 6.2%, $P = 0.16$), but significant for HT29 (12.4–5.7%, $P < 0.001$). CPT treatment did not induce any drastic effects on the repair efficiency of EcoRI-induced DSB, whatever cell lines tested (Figure 4B). Conversely, CPT treatment led to a significant decrease in the repair efficiency of plasmids with non-complementary ends for all cell lines (Figure 4C). Upon CPT treatment, the repair efficiency of non-complementary ends in HT29 decreased from 17.3% in untreated cells to 7.5% in cells treated with CPT ($P = 0.04$); it decreased by 8.7% in HCT116 cells (21 versus 12.3%, $P < 0.001$) and by 8% in LoVo cells (13.3 versus 5.3%, $P = 0.006$) in CPT-treated cells. In conclusion, while CPT treatment had no drastic effects on the repair efficiency of DSB with cohesive ends, treatment with this drug significantly impaired the ability of cells to repair DSB with non-complementary ends.

We have further determined the effects of CPT on the accuracy of repair (see Supplementary Material). With the exception of EcoRI-5′-PSS repair in HT29, where CPT treatment significantly increased the repair accuracy (48 versus 67.8%, $P = 0.007$), CPT did not modify the end-joining fidelity whatever cell lines and substrates tested. Thus, CPT treatment

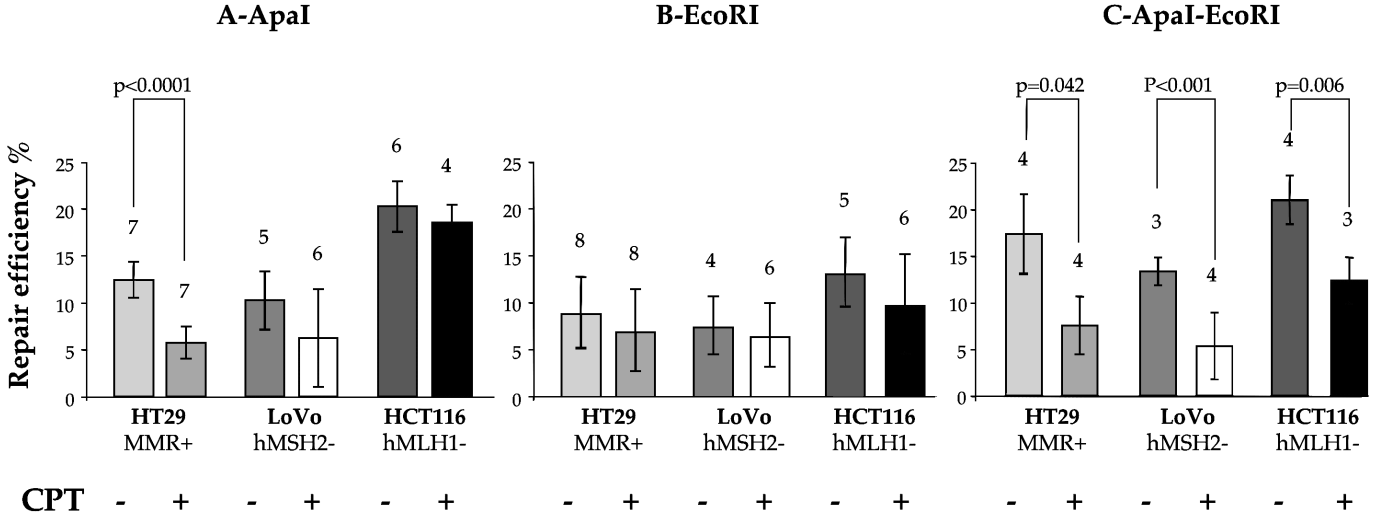

Figure 4. Effect of CPT treatment on DSB repair efficiency in CRC cell lines. Cells were treated with 100 nM CPT just after transfection and until plasmid recovery. Histograms represent the mean percentage of repair efficiency established from a minimum of three independent experiments for plasmids linearized with ApaI (**A**), EcoRI (**B**) and ApaI-EcoRI (**C**). The numbers of independent experiments are marked above each histogram for each CRC cell line tested. Only *P* values statistically different are specified.

Table 1. Detection of frameshift mutations in mononucleotide repeats in DNA damage signaling and repair genes

	ATR A10	BLM A9	BRCA1 A8	BRCA2 A8	DNA–PKcs A10	MRE11 T11	RAD50 A9
HT29	wt	wt	wt	wt	wt	wt	wt
LoVo	wt	−1*	wt	wt	wt	−1	−1/wt
HCT116	wt	wt	wt	wt	wt	−2/−1	−1/wt
DLD1	wt	wt	wt	wt	wt	−2*	wt

The presence of frameshift mutations in mononucleotide repeated sequences were searched in the MMR-proficient cell line HT29 and in the MMR-deficient cell lines HCT116, DLD1 and LoVo. The type and the length of the repeats are specified for each gene analyzed. WT, wild type indicates that no mutation could be detected in the mononucleotide tract. For each mutation, the number of base pair inserted (+) or deleted (−) is mentioned. Asterisk indicates the presence of a residual wt allele.

did not hamper the repair fidelity of accurate cell lines, including HCT116, LoVo or DLD1 cell lines.

Detection and analysis of frameshift mutations in DNA damage signaling and repair genes

In this study, we have observed significant differences in the repair fidelity of DSB with cohesive ends among cell lines, with the MMR-proficient HT29 cell line being the least accurate. Because neither the complementation of the hMLH1 defect in HCT116 nor the introduction of chromosome 2 in DLD1 affected the repair accuracy of substrates with cohesive ends, we concluded that the observed differences in end-joining fidelity could not be assigned to a direct influence of MMR. Thus, we have searched for frameshift mutations in mononucleotide repeats located within genes involved in DNA repair, DNA damage signaling and in the response of CPT treatment. In particular, we have studied the following coding repeats: *BRCA1* (A8), *BRCA2* (A8), *ATR* (A10), *DNA–PKcs* (A10), *BLM* (A9) and *RAD50* (A9) genes. We have performed the same analysis for the *MRE11* gene that carries an intronic T11 repeat whose mutation leads to aberrant splicing and synthesis of a truncated protein. As expected, no frameshift mutations in any of the genes could be detected in the MMR-proficient HT29 cell line (Table 1). None of the MMR-deficient cell lines displayed a mutation in *BRCA1*, *BRCA2*, *ATR* or *DNA–PKcs*. Mutations in *MRE11* were present in both alleles of all MMR-deficient cell lines tested. HCT116 displayed a bi-allelic mutation consisting of loss of 2 bp in one allele and loss of 1 bp in the other allele. In DLD1, the major form of *MRE11* corresponded to the loss of 2 bp, but the presence of a residual wild-type allele could be detected. LoVo showed a homozygous mutation consisting of 1 bp deletion. LoVo and HCT116 showed heterozygous mutations in *RAD50* and/or *BLM*, all consisting in the deletion of 1 bp in the A9 tracts.

DISCUSSION

The aim of our study is to investigate whether a defect in DSB repair by NHEJ could account for the hypersensitivity of MMR-deficient CRC cell lines to the cytotoxic effects of topoisomerase inhibitors. We have evaluated the efficiency and the accuracy of DSB repair in cell lines with various MMR defects, using an *in vivo* repair assay using plasmids linearized with restriction enzymes to generate cohesive or non-complementary ends. In this study, we have observed significant differences in the DSB repair efficiency among the cell lines tested, but the ability to perform efficient end-joining did not require a functional MMR system. As already reported in other studies using similar assays, the efficiency of repair of DSB with non-complementary ends was comparable to that of substrates with complementary 3′-PSS or 5′-PSS (20,21). Interestingly, we have observed that LoVo, as well as HCT116, DLD1 and their MMR-complemented counterparts are exquisitely accurate in end-joining DSB with cohesive ends, compared with the MMR-proficient HT29 cell line whose behavior was similar to that of various MMR-proficient cells, including CHO, normal human fibroblasts and normal human Epstein–Barr virus-transformed lymphoblastoid cell lines (20–24). Our observations are further reminiscent of a recent report performed with *Mlh1*-null mouse embryonic fibroblasts showing that Mlh1 does not influence the overall efficiency of DSB repair, but modulates error-prone NHEJ (25). The experimental system used in this study did not explore error-free repair, but revealed that rearrangements performed during NHEJ are less complex in *Mlh1*-deficient cells. This result is consistent with those obtained in our experiments, where the deletions accompanying error-prone events were significantly shorter in the MMR-deficient CRC cell lines than in HT29. However, as underlined by the authors, because *Mlh1* complementation of the *Mlh1*-null cells had not been tested, the possibility that other genetic factors might contribute to the differences observed in the NHEJ fidelity could not be formally excluded (25). In fact, our findings showing that the MMR-complemented counterparts of HCT116 and DLD1 behaved as their parental cells support the hypothesis of the involvement of other determinants favoring highly accurate DSB repair in these cells. The frameshift mutations that accumulate in a number of genes harboring repeated sequences, in MMR-deficient cells, persist in their MMR-complemented counterpart cells (26). This may explain why the MMR-complemented cells behave like their parental MMR-deficient cells. The extreme accuracy in DSB repair by NHEJ observed in the MMR-deficient cells and their complemented counterparts could be due to a decrease in the extent of degradation of the transfected plasmid. Alternatively, distinct mechanisms of NHEJ with variable accuracy contribute to repair DSB with cohesive ends. It has been shown in an *in vitro* study performed with extracts from human lymphoblastoid cells that Ku70, Ku86, DNA–PKcs and ligase IV/XRCC4 are required to repair DSB with cohesive and blunt ends, but antibodies against Ku and DNA–PKcs only partially inhibited the repair process, suggesting that this type of DSB can be repaired by an alternative pathway (27). Biochemical studies performed with human cell extracts recently demonstrated that the end-joining catalyzed by the ligase IV/XRCC4 complex can in fact occur by a distinct pathway that depends on the Mre11-Rad50-Nbs1 (M/R/N) complex and does not require DNA–PKcs (27,28). The respective contributions of these two NHEJ pathways, as well as their characteristics regarding the efficiency and the fidelity of repair have not been fully assessed yet. If the preferred pathways were influenced by the structure of DNA ends, it could explain why DNA–PKcs mutants are impaired in rejoining radiation-induced

DSB, but remain competent to repair etoposide-induced DSB or plasmids with cohesive ends (11,29). In keeping, our results showing that MMR-deficient cell lines carry inactivating mutations in *RAD50* and/or *MRE11* resulting in the under-expression of the M/R/N complex (data not shown) may explain why these cells are particularly accurate in repairing DSB with complementary ends. First, M/R/N participates in the exonucleolytic processing of DSB; in particular, it cleaves the 3′-PSS, such as those generated by ApaI, at the single- to double-strand transition (30,31). Second, in humans, the NHEJ pathway that depends on the M/R/N complex is an error-prone mechanism compared with the efficient and more accurate pathway that involves the Ku complex to protect ends from degradation prior to ligation (27).

Because MMR-deficient CRC cells are hypersensitive to topoisomerase inhibitors, we have evaluated the impact of CPT treatment on the efficiency and the fidelity of DSB repair. We have observed that CPT treatment has a mild effect on the repair efficiency of cohesive ends, but markedly decreases the ability of all cell lines to repair DSB with non-complementary ends, suggesting that repair of CPT-induced breaks may compete with that of non-complementary termini. While DSB caused by restriction enzymes possess complementary 4 bp overhangs that can be directly aligned and ligated, substrates with non-complementary ends, as well as CPT-induced DSB that have non-ligatable 5′OH/3′P termini, need to be processed to restore extremities competent for ligation. Several proteins, including BLM and the M/R/N complex, have been implicated in the processing of DSB with diverse structures. BLM, a 3′–5′ DNA helicase, has been reported to directly interact with hMLH1, to assemble with Ku70/Ku80 complex and DNA–PKcs near the site of DSB and to facilitate unwinding of DNA, promoting the alignment of microhomology elements during recombination (32–34). Interestingly, the sizes of the deletions that occur during inaccurate DSB repair in the absence of BLM are significantly smaller than in wild-type cells, similarly to what we have observed in the *hMLH1*-deficient cells. Moreover, the sequencing of error-prone events in the repair of complementary ends further showed that in the *MLH1*-deficient cell line, microhomology-mediated end-joining was less often used, as reported in *BLM*-deficient cells (data not shown) (33). Several observations suggest that the M/R/N complex may also play a substantial role in the repair of DSB with non-complementary termini, including CPT-induced DSB. Mre11 possesses a 3′–5′ exonuclease activity that is resumed when short sequence homologies, typically 1–5 bp long, are found, being then able to process to end-joining in the presence of ligase I or ligase IV *in vitro* (35). In *Saccharomyces cerevisiae*, the covalent complex formed by topoisomerase I and DNA may be removed using the 3′-endonuclease activity of Mre11 (9,36). In addition, M/R/N foci are formed in cells treated with CPT or etoposide, and Nbs1-deficient cells are highly sensitive to CPT (37–39). In that respect, it is noteworthy that in addition to *MRE11* and *RAD50*, *BLM* is also targeted by the MSI-driven mutagenesis characteristic of MMR-deficient cells.

In conclusion, our study does not provide evidence for a direct role of MMR components in the NHEJ-mediated repair of DSB created by restriction enzymes. The MMR defect may rather act through the accumulation of a number of MSI-driven mutations that inactivate microsatellite-harboring genes with key roles in damage signaling and/or repair of DNA damage, notably CPT-induced DNA lesions.

SUPPLEMENTARY MATERIAL

Supplementary Material is available at NAR Online.

ACKNOWLEDGEMENTS

CRC cell lines were kindly provided by Dr Peter Karran (Imperial Cancer Research Fund, Clare Hall, UK). DLD1-ch2 complemented cell line was kindly provided by Dr Thomas Kunkel (National Institute of Health, NC). The pHRecSJ plasmid used in this study was a generous gift from Dora Papadopoulo (UMR 218-CNRS, Institut Curie, Paris, France). We thank Prof. Pierre Netter, Dr Filippo Rosselli and the members of our laboratory for stimulating discussions. S.J. was supported by the Ministère de l'Education Nationale, de la Recherche et de la Technologie and the Ligue Nationale contre le Cancer. C.M. was supported by the Fondation pour la Recherche Médicale. This research was supported by grants from the Association pour la Recherche sur le Cancer (#4683), the Ligue Nationale contre le Cancer-Comité de Seine-et-Marne and the Groupement des Entreprises Françaises dans la Lutte contre le Cancer. Funding to pay the Open Access publication charges for this article was provided by the Association pour la Recherche sur le Cancer.

REFERENCES

1. Jacob,S., Aguado,M., Fallik,D. and Praz,F. (2001) The role of the DNA mismatch repair system in the cytotoxicity of the topoisomerase inhibitors camptothecin and etoposide to human colorectal cancer cells. *Cancer Res.*, **61**, 6555–6562.
2. Jiricny,J. and Nystrom-Lahti,M. (2000) Mismatch repair defects in cancer. *Curr. Opin. Genet. Dev.*, **10**, 157–161.
3. Wheeler,J.M., Bodmer,W.F. and Mortensen,N.J. (2000) DNA mismatch repair genes and colorectal cancer. *Gut*, **47**, 148–153.
4. Cunningham,J.M., Christensen,E.R., Tester,D.J., Kim,C.Y., Roche,P.C., Burgart,L.J. and Thibodeau,S.N. (1998) Hypermethylation of the hMLH1 promoter in colon cancer with microsatellite instability. *Cancer Res.*, **58**, 3455–3460.
5. Herman,J.G., Umar,A., Polyak,K., Graff,J.R., Ahuja,N., Issa,J.P., Markowitz,S., Willson,J.K., Hamilton,S.R., Kinzler,K.W. *et al.* (1998) Incidence and functional consequences of hMLH1 promoter hypermethylation in colorectal carcinoma. *Proc. Natl Acad. Sci. USA*, **95**, 6870–6875.
6. Fallik,D., Borrini,F., Boige,V., Viguier,J., Jacob,S., Miquel,C., Sabourin,J.C., Ducreux,M. and Praz,F. (2003) Microsatellite instability is a predictive factor of the tumor response to irinotecan in patients with advanced colorectal cancer. *Cancer Res.*, **63**, 5738–5744.
7. Pommier,Y., Pourquier,P., Fan,Y. and Strumberg,D. (1998) Mechanism of action of eukaryotic DNA topoisomerase I and drugs targeted to the enzyme. *Biochim. Biophys. Acta*, **1400**, 83–105.
8. Strumberg,D., Nitiss,J.L., Dong,J., Kohn,K.W. and Pommier,Y. (1999) Molecular analysis of yeast and human type II topoisomerases. Enzyme–DNA and drug interactions. *J. Biol. Chem.*, **274**, 28246–28255.
9. Pommier,Y., Redon,C., Rao,V.A., Seiler,J.A., Sordet,O., Takemura,H., Antony,S., Meng,L., Liao,Z., Kohlhagen,G. *et al.* (2003) Repair of and checkpoint response to topoisomerase I-mediated DNA damage. *Mutat. Res.*, **532**, 173–203.
10. Lees-Miller,S.P. and Meek,K. (2003) Repair of DNA double strand breaks by non-homologous end joining. *Biochimie*, **85**, 1161–1173.
11. Jin,S., Inoue,S. and Weaver,D.T. (1998) Differential etoposide sensitivity of cells deficient in the Ku and DNA–PKcs components of the DNA-dependent protein kinase. *Carcinogenesis*, **19**, 965–971.

12. Shao,R.G., Cao,C.X., Zhang,H., Kohn,K.W., Wold,M.S. and Pommier,Y. (1999) Replication-mediated DNA damage by camptothecin induces phosphorylation of RPA by DNA-dependent protein kinase and dissociates RPA:DNA–PK complexes. *EMBO J.*, **18**, 1397–1406.
13. Wu,J., Yin,M.B., Hapke,G., Toth,K. and Rustum,Y.M. (2002) Induction of biphasic DNA double strand breaks and activation of multiple repair protein complexes by DNA topoisomerase I drug 7-ethyl-10-hydroxy-camptothecin. *Mol. Pharmacol.*, **61**, 742–748.
14. Zhang,H., Richards,B., Wilson,T., Lloyd,M., Cranston,A., Thorburn,A., Fishel,R. and Meuth,M. (1999) Apoptosis induced by overexpression of hMSH2 or hMLH1. *Cancer Res.*, **59**, 3021–3027.
15. Wu,J., Gu,L., Wang,H., Geacintov,N.E. and Li,G.M. (1999) Mismatch repair processing of carcinogen-DNA adducts triggers apoptosis. *Mol. Cell. Biol.*, **19**, 8292–8301.
16. Harfe,B.D. and Jinks-Robertson,S. (2000) DNA mismatch repair and genetic instability. *Annu. Rev. Genet.*, **34**, 359–399.
17. Watanabe,Y., Haugen-Strano,A., Umar,A., Yamada,K., Hemmi,H., Kikuchi,Y., Takano,S., Shibata,Y., Barrett,J.C., Kunkel,T.A. *et al.* (2000) Complementation of an hMSH2 defect in human colorectal carcinoma cells by human chromosome 2 transfer. *Mol. Carcinog.*, **29**, 37–49.
18. Smith,J., Andrau,J.C., Kallenbach,S., Laquerbe,A., Doyen,N. and Papadopoulo,D. (1998) Abnormal rearrangements associated with V(D)J recombination in Fanconi anemia. *J. Mol. Biol.*, **281**, 815–825.
19. Birnboim,H.C. and Doly,J. (1979) A rapid alkaline extraction procedure for screening recombinant plasmid DNA. *Nucleic Acids Res.*, **7**, 1513–1523.
20. Escarceller,M., Buchwald,M., Singleton,B.K., Jeggo,P.A., Jackson,S.P., Moustacchi,E. and Papadopoulo,D. (1998) Fanconi anemia C gene product plays a role in the fidelity of blunt DNA end-joining. *J. Mol. Biol.*, **279**, 375–385.
21. Smith,J., Baldeyron,C., De Oliveira,I., Sala-Trepat,M. and Papadopoulo,D. (2001) The influence of DNA double-strand break structure on end-joining in human cells. *Nucleic Acids Res.*, **29**, 4783–4792.
22. Kabotyanski,E.B., Gomelsky,L., Han,J.O., Stamato,T.D. and Roth,D.B. (1998) Double-strand break repair in Ku86- and XRCC4-deficient cells. *Nucleic Acids Res.*, **26**, 5333–5342.
23. Merel,P., Prieur,A., Pfeiffer,P. and Delattre,O. (2002) Absence of major defects in non-homologous DNA end joining in human breast cancer cell lines. *Oncogene*, **21**, 5654–5659.
24. Smith,J., Riballo,E., Kysela,B., Baldeyron,C., Manolis,K., Masson,C., Lieber,M.R., Papadopoulo,D. and Jeggo,P. (2003) Impact of DNA ligase IV on the fidelity of end joining in human cells. *Nucleic Acids Res.*, **31**, 2157–2167.
25. Bannister,L.A., Waldman,B.C. and Waldman,A.S. (2004) Modulation of error-prone double-strand break repair in mammalian chromosomes by DNA mismatch repair protein Mlh1. *DNA Repair (Amst.)*, **3**, 465–474.
26. Duval,A. and Hamelin,R. (2002) Mutations at coding repeat sequences in mismatch repair-deficient human cancers: toward a new concept of target genes for instability. *Cancer Res.*, **62**, 2447–2454.
27. Baumann,P. and West,S.C. (1998) DNA end-joining catalyzed by human cell-free extracts. *Proc. Natl Acad. Sci. USA*, **95**, 14066–14070.
28. Udayakumar,D., Bladen,C.L., Hudson,F.Z. and Dynan,W.S. (2003) Distinct pathways of nonhomologous end joining that are differentially regulated by DNA-dependent protein kinase-mediated phosphorylation. *J. Biol. Chem.*, **278**, 41631–41635.
29. Cheong,N., Perrault,A.R., Wang,H., Wachsberger,P., Mammen,P., Jackson,I. and Iliakis,G. (1999) DNA–PK-independent rejoining of DNA double-strand breaks in human cell extracts *in vitro*. *Int. J. Radiat. Biol.*, **75**, 67–81.
30. Paull,T.T. and Gellert,M. (1998) The 3′ to 5′ exonuclease activity of Mre 11 facilitates repair of DNA double-strand breaks. *Mol. Cell*, **1**, 969–979.
31. Paull,T.T. and Gellert,M. (1999) Nbs1 potentiates ATP-driven DNA unwinding and endonuclease cleavage by the Mre11/Rad50 complex. *Genes Dev.*, **13**, 1276–1288.
32. Langland,G., Kordich,J., Creaney,J., Goss,K.H., Lillard-Wetherell,K., Bebenek,K., Kunkel,T.A. and Groden,J. (2001) The Bloom's syndrome protein (BLM) interacts with MLH1 but is not required for DNA mismatch repair. *J. Biol. Chem.*, **276**, 30031–30035.
33. Langland,G., Elliott,J., Li,Y., Creaney,J., Dixon,K. and Groden,J. (2002) The BLM helicase is necessary for normal DNA double-strand break repair. *Cancer Res.*, **62**, 2766–2770.
34. Onclercq-Delic,R., Calsou,P., Delteil,C., Salles,B., Papadopoulo,D. and Amor-Gueret,M. (2003) Possible anti-recombinogenic role of Bloom's syndrome helicase in double-strand break processing. *Nucleic Acids Res.*, **31**, 6272–6282.
35. Paull,T.T. and Gellert,M. (2000) A mechanistic basis for Mre11-directed DNA joining at microhomologies. *Proc. Natl Acad. Sci. USA*, **97**, 6409–6414.
36. D'Amours,D. and Jackson,S.P. (2002) The Mre11 complex: at the crossroads of dna repair and checkpoint signalling. *Nature Rev. Mol. Cell. Biol.*, **3**, 317–327.
37. Maser,R.S., Monsen,K.J., Nelms,B.E. and Petrini,J.H. (1997) hMre11 and hRad50 nuclear foci are induced during the normal cellular response to DNA double-strand breaks. *Mol. Cell. Biol.*, **17**, 6087–6096.
38. Kraakman-van der Zwet,M., Overkamp,W.J., Friedl,A.A., Klein,B., Verhaegh,G.W., Jaspers,N.G., Midro,A.T., Eckardt-Schupp,F., Lohman,P.H. and Zdzienicka,M.Z. (1999) Immortalization and characterization of Nijmegen Breakage syndrome fibroblasts. *Mutat. Res.*, **434**, 17–27.
39. Habraken,Y., Jolois,O. and Piette,J. (2003) Differential involvement of the hMRE11/hRAD50/NBS1 complex, BRCA1 and MLH1 in NF-kappaB activation by camptothecin and X-ray. *Oncogene*, **22**, 6090–6099.